iScience, Volume *25*

Supplemental information

Crystal growth engineering and origin of the weak ferromagnetism in antiferromagnetic matrix of orthochromates from *t*-*e* orbital hybridization

Yinghao Zhu, Junchao Xia, Si Wu, Kaitong Sun, Yuewen Yang, Yanling Zhao, Hei Wun Kan, Yang Zhang, Ling Wang, Hui Wang, Jinghong Fang, Chaoyue Wang, Tong Wu, Yun Shi, Jianding Yu, Ruiqin Zhang, and Hai-Feng Li

Supplementary Information
Crystal growth engineering and origin of the weak ferromagnetism in antiferromagnetic matrix of orthochromates from *t*-*e* orbital hybridization

Yinghao Zhu[a,b,c,d,1], Junchao Xia[a,d,1], Si Wu[a,d,1], Kaitong Sun[a], Yuewen Yang[b], Yanling Zhao[b], Hei Wun Kan[b], Yang Zhang[c], Ling Wang[c], Hui Wang[c], Jinghong Fang[c], Chaoyue Wang[c], Tong Wu[c], Yun Shi[c], Jianding Yu[c,*], Ruiqin Zhang[b,*], Hai-Feng Li[a,2,*]

[a] *Joint Key Laboratory of the Ministry of Education, Institute of Applied Physics and Materials Engineering, University of Macau, Avenida da Universidade, Taipa, Macao SAR, 999078, China*
[b] *Department of Physics, City University of Hong Kong, Kowloon, Hong Kong SAR, 999077, China*
[c] *State Key Laboratory of High Performance Ceramics and Superfine Microstructure, Shanghai Institute of Ceramics, Chinese Academy of Sciences, Shanghai, 200050, China*
[d] *Guangdong–Hong Kong–Macao Joint Laboratory for Neutron Scattering Science and Technology, No. 1. Zhongziyuan Road, Dalang, DongGuan, 523803, China*

Abstract

Supplemental Figures S1~S4 and supplemental Tables S1~S3.

[*] Corresponding author
Email addresses: yujianding@mail.sic.ac.cn (Jianding Yu), aprqz@cityu.edu.hk (Ruiqin Zhang), haifengli@um.edu.mo (Hai-Feng Li)
[1] These authors contributed equally.
[2] Lead Author.

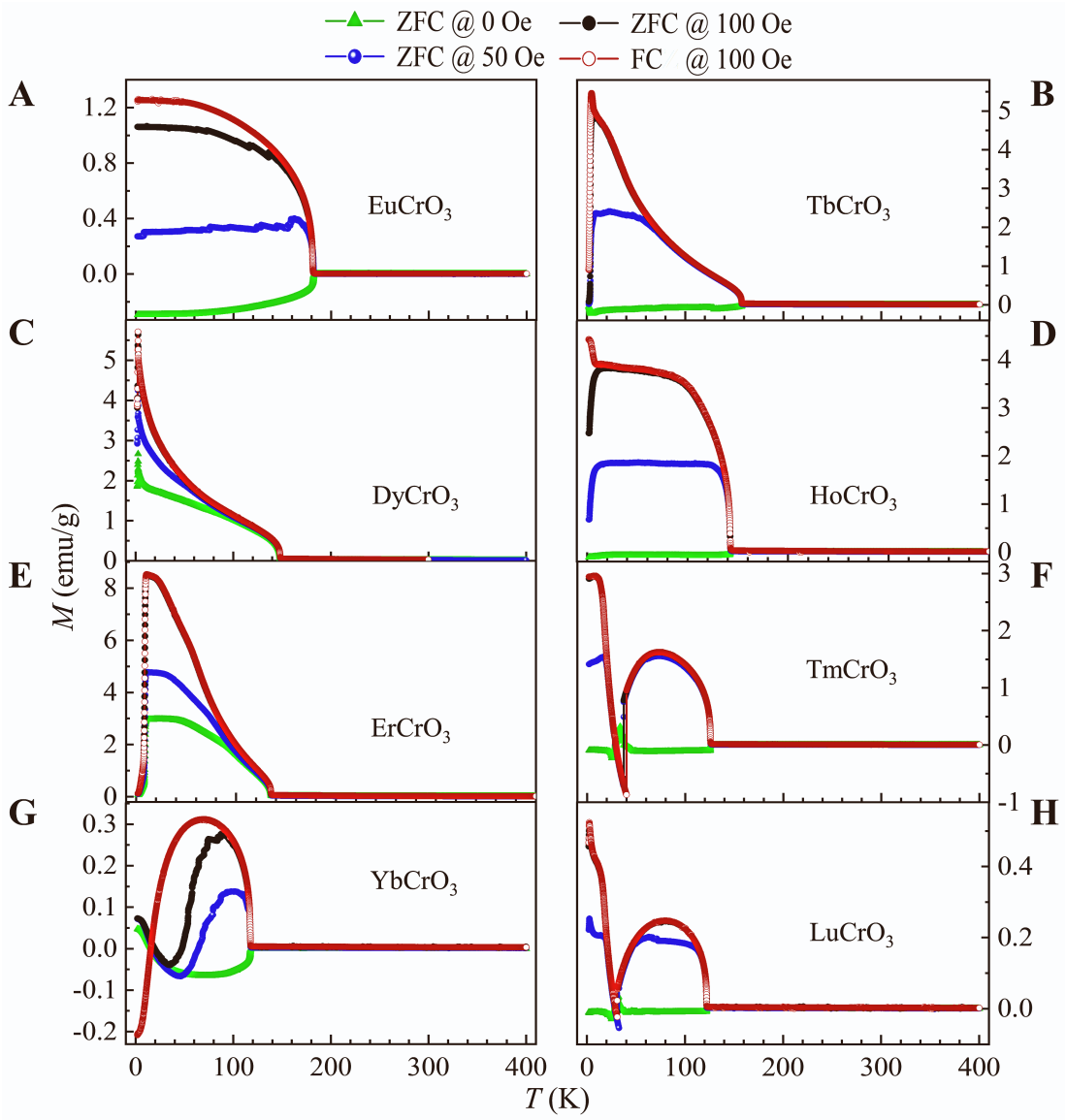

Figure S1. Temperature dependent magnetization data in the entire studied temperature range of 1.8–400 K, measured at 0, 50, and 100 Oe. No additional features were observed in the temperature range of 200–400 K. (A) $EuCrO_3$, (B) $TbCrO_3$, (C) $DyCrO_3$, (D) $HoCrO_3$, (E) $ErCrO_3$, (F) $TmCrO_3$, (G) $YbCrO_3$, and (H) $LuCrO_3$. We performed both zero-field and field-cooling measurements at 100 Oe.
Related to Figure 3A, Figure 4A, Figure 5A, Figure 5B, Figure 6A, Figure 7A, Figure 8A, Figure 9A, and Figure 10A.

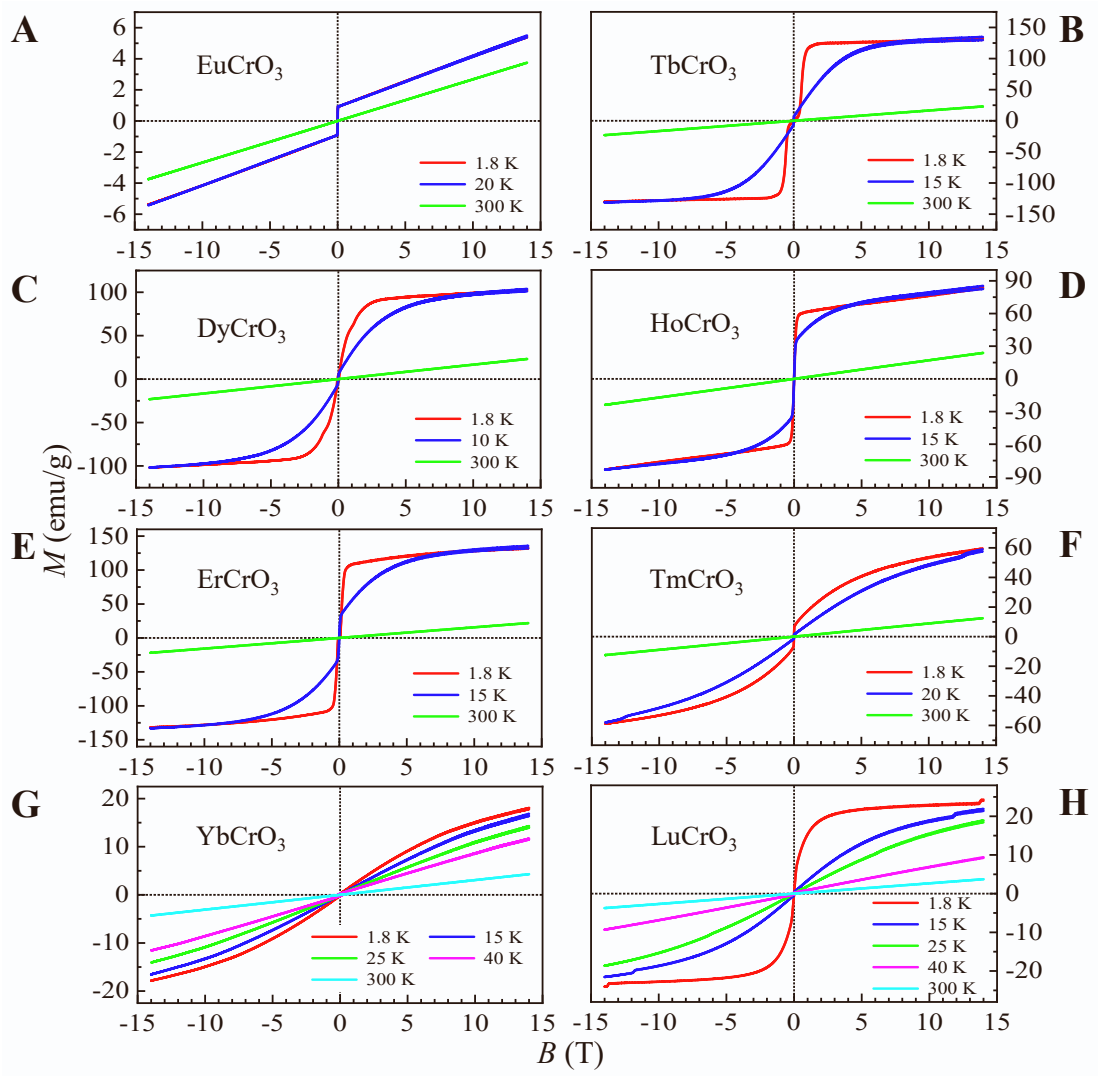

Figure S2. Applied magnetic-field dependent magnetization data in the whole studied field range from −14 to 14 T at selected temperatures. Here we can see the magnetization evolution as the applied magnetic field increases. For example, when does the magnetization plateaus? What is the strength of the measured magnetization at 1.8 K and 14 T? (A) $EuCrO_3$, (B) $TbCrO_3$, (C) $DyCrO_3$, (D) $HoCrO_3$, (E) $ErCrO_3$, (F) $TmCrO_3$, (G) $YbCrO_3$, and (H) $LuCrO_3$. We carried out the measurements in a zero-field cooling mode.
Related to Figure 3C, Figure 4C, Figure 5D, Figure 6C, Figure 7C, Figure 8C, Figure 9C, and Figure 10C.

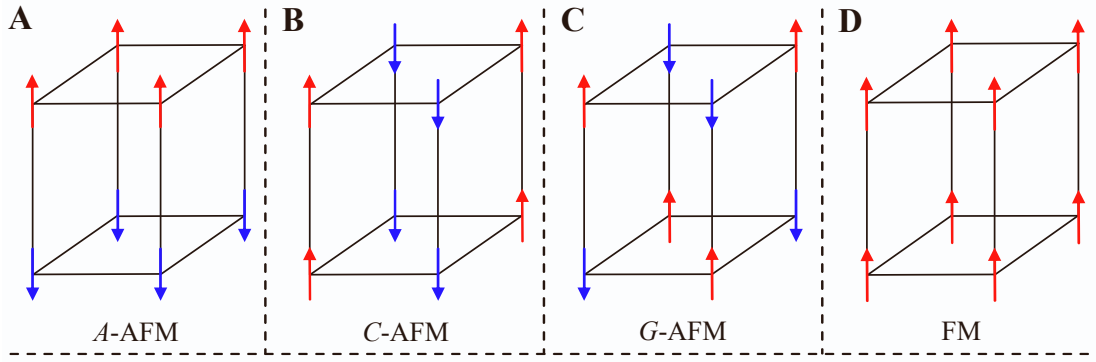

Figure S3. The potential four-types of magnetic structures for orthochromates at low temperatures. We optimized their total energies and listed the results in Table S3. We took the energy value of the *G*-type antiferromagnetic structure as the energy baseline (= 0 meV). It is clear that all other types of magnetic structure have much higher energy levels than that of the *G*-type one. Therefore, we conclude that the *G*-type antiferromagnetic structure is the most stable one for $RECrO_3$ (RE = Y, Eu, Gd, Tb, Dy, Ho, Er, Tm, Yb, and Lu) orthochromates. (A) *A*-type, (B) *C*-type, and (C) *G*-type antiferromagnetic structures. (D) The ferromagnetic structure. The two types of arrows drawn in Figure S3A-S3D represent the two spin sublattices.
Related to Tables 2 and 3 and Discussion.

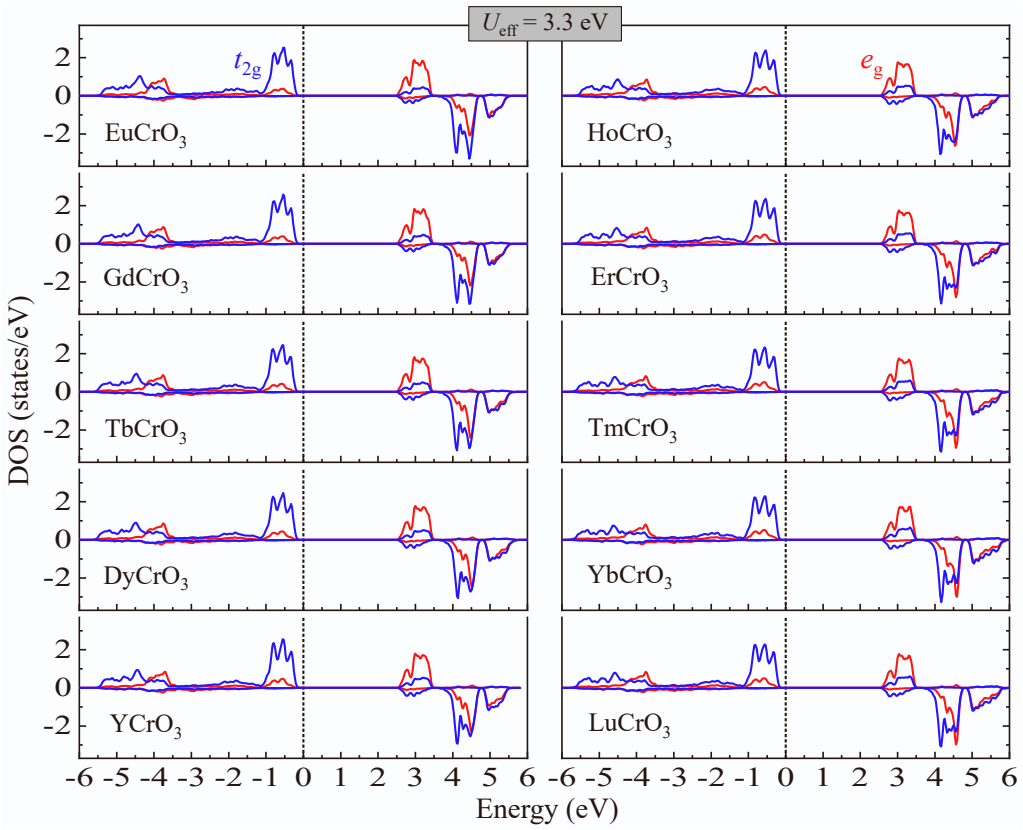

Figure S4. Calculated density of states (DOSs) of t_{2g} and e_g orbitals (as marked) of Cr^{3+} ions in $RECrO_3$ (RE = Eu, Gd, Tb, Dy, Y, Ho, Er, Tm, Yb, and Lu) at U_{eff} = 3.3 eV. The positive and negative values denote high- and low-spin states, respectively. The vertical short-dotted lines at energy = 0 eV represent the Fermi level. Here the *t*-*e* orbital hybridization is obvious above the Fermi level.
Related to Table 3 and Discussion.

Table S1 Calculated structural parameters (lattice constants, unit-cell volume, atomic positions, bond lengths, and bond angles) of $RECrO_3$ (RE = Y, Eu, Gd, Tb, and Dy) compounds. These were optimized theoretically by density-of-state calculations. The ionic radii (IR) of RE^{3+} ions and the Wyckoff sites of all atoms were also included. We calculated values of the tolerance factor *t*.
Related to Table 3 and Figure 12.

Theoretically optimized structural parameters of $RECrO_3$ compounds (Orthorhombic, space group: *Pbnm* (No. 62), $Z = 4$)					
RE =	Y	Eu	Gd	Tb	Dy
IR (RE^{3+}) (Å)	1.040	1.087	1.078	1.063	1.052
tolerance factor *t*	0.8081	0.8248	0.8216	0.8163	0.8124
a (Å)	5.2528	5.3184	5.2999	5.2682	5.2462
b (Å)	5.5761	5.6054	5.5845	5.5844	5.5788
c (Å)	7.5737	7.6416	7.6232	7.5882	7.5705
V (Å^3)	221.837	227.806	225.624	223.241	221.567
$\alpha = \beta = \gamma$ (°)	90	90	90	90	90
Cr-O1 (Å)	1.9866	1.9872	1.9864	1.9841	1.9839
Cr-O2 (Å)	2.0030	2.0034	2.0012	2.0021	2.0011
Cr-O2 (Å)	2.0059	2.0108	2.0057	2.0053	2.0032
⟨Cr-O⟩ (Å)	1.9985	2.0005	1.9978	1.9972	1.9961
∠Cr-O1-Cr (°)	144.78	148.03	147.25	145.93	145.11
∠Cr-O2-Cr (°)	145.67	148.50	147.78	146.62	145.96
⟨∠Cr-O-Cr⟩ (°)	145.37	148.34	147.60	146.39	145.68
RE (4*c*)					
x	−0.0189	−0.0171	−0.0176	−0.0185	−0.0191
y	0.0701	0.0671	0.0662	0.0691	0.0704
z			0.25		
Cr (4*b*)					
(*x*, *y*, *z*)			(0.00, 0.00, 0.50)		
O1 (4*c*)					
x	0.1078	0.0982	0.1005	0.1045	0.1071
y	0.4638	0.4709	0.4691	0.4667	0.4651
z			0.25		
O2 (8*d*)					
x	−0.3079	−0.3020	−0.3034	−0.3068	−0.3081
y	0.3018	0.2977	0.2987	0.3010	0.3017
z	0.0551	0.0505	0.0517	0.0528	0.0540

Table S2 Calculated structural parameters (lattice constants, unit-cell volume, atomic positions, bond lengths, and bond angles) of $RECrO_3$ (RE = Ho, Er, Tm, Yb, and Lu) compounds. These were optimized theoretically by density-of-state calculations. The ionic radii (IR) of RE^{3+} ions and the Wyckoff sites of all atoms were also included. We calculated values of the tolerance factor *t*.
Related to Table 3 and Figure 12.

Theoretically optimized parameters of $RECrO_3$ compounds (Orthorhombic, space group: *Pbnm* (No. 62), $Z = 4$)					
RE =	Ho	Er	Tm	Yb	Lu
IR (RE^{3+}) (Å)	1.041	1.030	1.020	1.008	1.001
tolerance factor *t*	0.8085	0.8046	0.8010	0.7968	0.7943
a (Å)	5.2249	5.2092	5.1952	5.1808	5.1958
b (Å)	5.5735	5.5651	5.5484	5.5328	5.5504
c (Å)	7.5514	7.5283	7.5120	7.5047	7.5076
V (Å^3)	219.905	218.244	216.533	215.116	216.508
$\alpha = \beta = \gamma$ (°)	90	90	90	90	90
Cr-O1 (Å)	1.9857	1.9851	1.9852	1.9864	1.9850
Cr-O2 (Å)	1.9996	1.9991	1.9953	1.9925	1.9948
Cr-O2 (Å)	2.0031	2.0018	2.0026	1.9994	2.0032
⟨Cr-O⟩ (Å)	1.9961	1.9953	1.9944	1.9928	1.9943
∠Cr-O1-Cr (°)	143.88	142.92	142.17	141.65	142.00
∠Cr-O2-Cr (°)	145.22	144.59	143.85	143.39	143.92
⟨∠Cr-O-Cr⟩ (°)	144.77	144.03	143.29	142.81	143.28
RE (4*c*)					
x	−0.0199	−0.0204	−0.0216	−0.0217	−0.0209
y	0.0714	0.0725	0.0743	0.0746	0.0739
z			0.25		
Cr (4*b*)					
(*x*, *y*, *z*)			(0.00, 0.00, 0.50)		
O1 (4*c*)					
x	0.1105	0.1131	0.1162	0.1182	0.1162
y	0.4616	0.4593	0.4599	0.4594	0.4585
z			0.25		
O2 (8*d*)					
x	−0.3093	−0.3105	−0.3107	−0.3114	−0.3115
y	0.3026	0.3033	0.3042	0.3047	0.3049
z	0.0555	0.0568	0.0588	0.0596	0.0578

Table S3 Total energy of each $RECrO_3$ compound with the *A*-type, *C*-type, and *G*-type antiferromagnetic structures and the ferromagnetic structure. We took the *G*-type antiferromagnetic state as the energy baseline. The unit of the total energy is meV per formula. Related to Discussion.

	A-AFM	*C*-AFM	*G*-AFM	FM
$EuCrO_3$	22.8	9.5	0	38.5
$GdCrO_3$	21.0	9.0	0	35.5
$TbCrO_3$	19.5	7.5	0	32.5
$DyCrO_3$	18.5	6	0	30.0
$YCrO_3$	12.7	5.5	0	27.3
$HoCrO_3$	17.8	4.3	0	26.8
$ErCrO_3$	17.0	3.3	0	24.8
$TmCrO_3$	16.3	2.8	0	23.8
$YbCrO_3$	16.8	1.0	0	22.3
$LuCrO_3$	17.0	2.0	0	23.5